Polymer hydrogel functionalized with biodegradable nanoparticles as composite system for controlled drug delivery

Filippo Rossi[1], **Raffaele Ferrari**[1], **Franca Castiglione, Andrea Mele, Giuseppe Perale and Davide Moscatelli**

Dipartimento di Chimica, Materiali e Ingegneria Chimica 'Giulio Natta', Politecnico di Milano, via Mancinelli 7, 20131 Milano, Italy

E-mail: davide.moscatelli@polimi.it

Received 1 July 2014, revised 21 September 2014
Accepted for publication 6 October 2014
Published 9 December 2014

1. Introduction

Research in the area of controlled drug delivery systems has gained increasing importance in approximately the last 20 years due to the advantages in terms of safety, efficacy and patient convenience that these long-acting systems are able to provide [1–3]. Traditional methods of drug administration in conventional forms, such as pills and subcutaneous or intravenous injections, offer limited control over the rate of drug release into the body, and they are associated with an immediate uncontrolled burst release of drugs [4, 5]. Consequently, to achieve therapeutic levels, the initial concentration of the drug in the body must be high, causing peaks that gradually diminish over time to an ineffective level [4, 6]. Then, the main purpose behind controlled drug delivery is to provide an optimal drug administration, avoiding under- and overdosing and maintaining drug levels within a desired range over a long period with a diminished amount of administered drugs [7, 8]. Recent advances in polymer science have provided a huge amount of innovations; in particular, polymer nanoparticles (NPs) are gaining increasing interest due to their flexibility in terms of size, hydrophilic/hydrophobic characteristics and surface functionalization [9–11]. They offer relevant advantages in drug delivery by targeting molecules in specific cells and controlling drug release over time. In particular, several recent studies underlined their ability to target

[1] These authors equally contributed to this work.

specific cells to provide selective drug treatments [12–16]. The direct injection of a colloidal NP suspension is a good option, but several concerns arise: injected NPs very often leave the zone of injection as they are not confined by any support and easily extravasate into the circulatory torrent, migrating all over the body to the liver and the spleen or toward an uncertain fate [17]. According to these critical issues, nanostructured hydrogels synthesized from polycondensation between agarose and carbomer 974p (AC) could be reliable NP carriers due to their ability to control release rates *in situ* [18, 19]. In this direction we recently demonstrated the selective efficacy of minocycline once loaded in biodegradable NPs and injected *in situ* using cross-linked hydrogels to reduce the inflammatory response mediated by microglia/macrophage activation in a spinal cord injury [20, 21]. Therefore, on the one hand, the possibility to selectively address drug treatments is universally known as one of the main novelties in the field [22, 23]; on the other hand, the possibility to deliver drugs to not only macrophages is an attractive alternative for pharmacological treatments [24–27].

Following this viewpoint we investigated the possibility to functionalize hydrogels with drug-loaded polymer NPs, creating a novel composite material able to guarantee: (i) the possibility to remain localized at the site of injection, (ii) the sustained release kinetics of hydrophobic drugs and (iii) the release of drugs directed not only to macrophages.

Recently, composite materials combining hydrogel and polymer NPs in one system have been reported in literature; however, they are mainly constituted by scaffolds from nanogels aggregations [28, 29] or based on drug-loaded NPs entrapped into a pre-formed hydrogel with the aim to tailor the release rate of the adopted drugs [30, 31]. To the best of our knowledge, no work appeared regarding the conjunction through covalent bonds of these two systems in one single device able to remain localized at the site of injection (typical of hydrogels) and release hydrophobic drugs with sustained release rates (typical of NPs), avoiding the quick cell uptake [32]. Polymeric NPs are obtained through a two-step process. Polymer chains constituting NPs possess a peculiar comb-like structure in which a poly(2-hydroxy-ethyl methacrylate) backbone is grafted with poly-ε-caprolactone (PCL) and poly (ethylene glycol) (PEG) chains controllable in terms of both length and composition [33, 34]. The selected hydrogel, specifically developed for *in situ* repair strategies, was obtained from a statistical block polycondensation reaction between agarose and carbomer 974P, together with NPs [20, 35]. NP functionalization within the hydrogel was studied with Fourier transform infrared spectroscopy (FTIR) and high resolution magic angle spinning-nuclear magnetic resonance (HRMAS-NMR) and by investigating the release kinetics from the hydrogel matrix. Moreover, the physical chemical properties of the composite material were evaluated together with the ability to sustain the delivery of a mimetic drug compound (To-Pro3). This represents a good proof of concept of the possibility not only to selectively direct drug treatment to cell lines but also to release compounds all along the damaged tissue.

2. Materials and methods

2.1. Materials

For the macromonomer synthesis ε-caprolactone (CL, 99%), 2-hydroxyethyl methacrylate (HEMA, ⩾99%) and 2-ethylhexanoic acid tin(II) salt ($Sn(Oct)_2$, ~95%) were all purchased from Sigma-Aldrich (Germany) and used without further treatment. For the NP synthesis potassium persulfate (KPS; ⩾99%), poly(ethylene glycol) methacrylate (HEMA-PEG_9, Molecular weight: about 526 Da) and polyoxyethylene sorbitan monooleate (Tween80®) were purchased from Sigma-Aldrich (Germany) and used without further treatment. For size exclusion chromatography (SEC) analysis THF (⩾99.7%, Sigma) was used as the eluent. For hydrogel synthesis, cross-linked poly(acrylic acid) carbomer 974P was purchased by Fagron (The Netherlands), agarose was purchased from Invitrogen (Carlsbad, CA, USA) and the phosphate buffered saline solution (PBS), propylene glycol, glycerol and sodium hydroxide were purchased from Sigma-Aldrich (Germany) and used as received.

2.2. Synthesis and characterization of HEMA-CL_3 macromonomers

The macromonomers used for NP synthesis were obtained through a ring opening polymerization (ROP) reaction using a procedure reported in the literature [34]. The reaction was carried out in bulk conditions without using any solvent. 10 g of CL were heated up in a stirred flask at 130 ± 1 °C, with the temperature controlled by an external oil bath. A mixture of $Sn(Oct)_2$ and HEMA at a given molar ratio (1/400) was prepared and left under continuous magnetic stirring at room temperature until the complete dissolution of $Sn(Oct)_2$. Then, a HEMA solution (composed of 3.8 g of HEMA and 29 mg of $Sn(Oct)_2$) was then added to the CL (CL/HEMA molar ratio equal to 3) to initiate the reaction, which was carried out for two hours. The reaction product on the HEMA molecule functionalized with 3 units of caprolactone, here reported as HEMA-CL_3, was refrigerated at 4 °C, awaiting further use. The macromonomer molecular weight (MW) and thus the average chain length *n* (the average number of CL units added to the HEMA molecule, theoretically equal to 3 in this work) characterization was carried out combining SEC with ^{1}H-NMR analysis. For SEC analysis, THF was used as the eluent with a 0.5 mL min^{-1} flow rate and a temperature of 35 °C.

The instrument (Agilent, 1100 series, Germany) was equipped with two detectors in the series (ultraviolet (UV) and differential refractive index (RI)), three PLgel columns (Polymer laboratories Ltd, UK; two with pore sizes of MXC type and one oligopore; length of 300 mm and 7.5 mm ID) and a pre-column.

Universal calibration was applied based on polystyrene standards from 580 Da to 3250 000 Da (Polymer Laboratories) and using Mark–Houwink parameters for HEMA-CL_n ($K = 2.00 \times 10^{-4}$ [dL/g] and $a = 0.571$ [-]) [34]. H-NMR was performed using a 500 MHz Ultrashield NMR spectrometer (Bruker, Switzerland) by dissolving the sample in $CDCl_3$.

2.3. Synthesis of poly(HEMA-g-CL_3-PEG_9)-based nanoparticles

The procedure involved in the production of PEGylated PCL-based NPs involves a two-step process. Firstly, short PCL oligomers with a targeted chain length functionalized with a vinyl end group have been produced through a ring opening polymerization reaction, as explained in the previous section. This polymerizable compound has been used in a monomer-starved semibatch emulsion polymerization (MSSEP) process in order to produce final NPs composed by a comb-like polymer, as reported already in literature [36]. Here, the production of NPs via MSSEP using HEMA-CL_3 copolymerized with HEMA-PEG_9 is described. The polymerization of the produced macromonomers was carried out in a 50 mL three-neck glass flask. This procedure consists of the loading of the more hydrophilic monomer (in this case, HEMA-PEG_9), together with 0.125 g of Tween80, in the reactor as in a normal batch reaction, while the more hydrophobic monomer is injected as in a semi-batch process. More in detail 0.29 g of HEMA-PEG_9 were added to 50 mL of distilled water, and the solution was heated up to 80 °C, while an inert atmosphere was obtained after vacuum-nitrogen cycles. 0.02 g of KPS were added to the purged solution. After that, 2.21 g of the HEMA-CL_3 macromonomer were injected with a rate of 2 mL h^{-1} using a syringe pump (Model NE-300, New Era Pump System, US). The reaction was run for three hours. The total amount of injected macromonomer was 2.5 g, giving a solid content in the final latex equal to 5% w/w.

The mass ratio of the two macromonomers was selected in order to maintain their molar ratio, the parameter *r*, as equal to 1/8.

2.4. Characterization of poly(HEMA-g-CL_3-PEG_9)-based nanoparticles: DLS and TEM analyses

The final particle size was determined by dynamic light scattering (DLS) (Malvern, Zetanano ZS, US); the analyses were performed in triplicate, and the reported data are the average of three runs in which the standard deviation was always below 5%. The dimension and morphology of the produced NPs were also confirmed by transmission electron microscopy (TEM) using an EFTEM Leo 912AB at 80 kV, Karl Zeiss, Jena, Germany).

The samples were prepared placing a 5 μL drop of NP dispersion on a Formvar/carbon-coated copper grid and dried overnight. The digital images were acquired by a charge coupled device ((CCD), Esi Vision Proscan camera).

2.5. Synthesis of agarose-carbomer-based hydrogels and NP loading

2.5.1. AC synthesis. Hydrogels were prepared by batch reaction in a PBS at about 80 °C in which a polymeric solution was achieved by stirring polymers (1% w/v carbomer 974p and 0.5% w/v agarose) into the selected solvent, adding a mixture of cross-linking agents made of propylene glycol and glycerol (along with NaOH 1 N for pH neutralization) [20, 37]. The reaction pH was indeed kept neutral. The effective gelation and reticulation were achieved by means of electromagnetic stimulation (500 W power irradiated) for 15 s min per 5 mL of polymeric solution. The mixing reactor was kept closed to avoid any eventual loss of solvent vapors, and the gelation was then achieved in a 48 multiwell cell culture plate (0.5 mL each with the cylinder diameter of 1.1 cm) in which the gelling solution was poured during cooling. Then, the hydrogels were washed with PBS to remove the unreacted cross-linkers.

2.5.2. NP-loaded hydrogel (p-AC) synthesis. During the AC hydrogel cooling phase, which was slightly above 37 °C, the AC samples were homogenously mixed with a water suspension of NPs, with a final NP concentration of 1% (w/v macromonomer/solvent).

This procedure allows loading NPs during the sol state before the sol/gel transition takes place. Gelation was then achieved in a 48 multiwell cell culture plate (0.5 mL each with the cylinder diameter of 1.1 cm) in which the gelling solution was poured during cooling. Then, the hydrogels were washed with an isotonic solution of NPs to remove the unreacted cross-linkers, avoiding the NPs release.

2.5.3. NP functionalized hydrogel (f-AC) synthesis. NPs were used as cross-linkers, instead of diols and thiols (glycerol and propylene glycol), with polymers (carbomer 974p and agarose). The composition used in the PBS was 1% carbomer 974P and 0.5% agarose, along with NaOH 1 N, to reach pH = 7.4; then, the composition was homogenously mixed with a NP water suspension with a final NP concentration of 1% (w/v macromonomer/solvent). Effective gelation and reticulation were achieved by means of electromagnetic stimulation (500 W power irradiated) for 15 s min per 5 mL of polymeric solution.

The mixing reactor was kept closed to avoid any eventual loss of solvent vapors, and the gelation was then achieved in a 48 multiwell cell culture plate (0.5 mL each with the cylinder diameter of 1.1 cm) where the gelling solution was poured during cooling. Then, hydrogels were washed with an isotonic solution of NPs to remove the unreacted cross-linkers, avoiding the NPs release.

2.6. Characterization of agarose-carbomer-based hydrogels: FTIR and HRMAS-NMR spectroscopy

Hydrogel samples, after being left to soak in excess of the PBS, were freeze-dried and laminated with potassium bromide. The FTIR spectra were recorded using a Thermo Nexus 6700 spectrometer coupled to a Thermo Nicolet Continuum microscope with a ×15 Reflachromat Cassegrain objective. The ^{1}H and ^{13}C NMR spectra of hydrogel p-AC and f-AC were recorded on a Bruker Avance spectrometer operating at a 500 MHz proton frequency and equipped with a dual $^{1}H/^{13}C$ HRMAS probe head for semi-solid samples. The samples were swollen in D_2O and transferred in a 4 mm ZrO_2 rotor containing a volume of about 50 μL. All of the spectra were acquired at room temperature with a spinning rate of 4 kHz to eliminate the dipolar contribution. Liquid-state ^{1}H

and ^{13}C NMR spectra of the monomers dissolved in $CDCl_3$ were recorded on a Bruker Avance spectrometer operating at a 500 MHz proton frequency and equipped with a QNP four nuclei switchable probe. The ^{1}H-^{13}C 2D HSQC (heteronuclear single quantum coherence) experiment was performed with $ns = 16$ and $TD = 512$ in the F2 dimension.

2.7. NP release from hydrogels

The NPs release from p-AC was compared with f-AC: p-AC and f-AC were cast in standard plastic 48-well cell culture plates (0.5 mL/well). Once gelified, both the p-AC and f-AC systems were transferred in standard plastic 6-well cell culture plates [38]. Complete swelling, without release, was achieved, leaving samples in an isotonic solution with NPs within a standard incubator at 37 °C and in a 5% CO_2 atmosphere overnight. The stability of these materials was found to be quite high. Indeed, they remain stable for weeks before significant degradation by hydrolysis takes place [38]. The degradation reactions can be fully neglectable in this work since its characteristic time is much greater than the experiment length. Therefore, the NP flux is controlled only by the concentration gradient, and the diffusion can be considered as Fickian. After one day, the hydrogels were placed in PBS-filled wells (5 mL volume each).

The aliquots were collected at defined time points, and the sample volume was replaced by fresh PBS in order to avoid mass-transfer equilibrium between the gel and the surrounding solution. The samples collected were analyzed to assess the NP-released fraction using DLS (Supporting Information) [38].

2.8. Gelation time and swelling behavior

Gelation time was assessed using the inverted test tube [39]. To assess the swelling kinetics, hydrogel samples were first immersed in PBS for about 24 h, then freeze-dried, weighted (W_d) and poured in excess of the PBS to achieve complete swelling at 37 °C in a 5% CO_2 atmosphere. The swelling kinetics were measured gravimetrically: samples were removed from the PBS at regular time points. Then, hydrogel surfaces were wiped with moistened filter paper in order to remove the excess PBS and then weighed (W_t). The swelling ratio is defined as follows

$$swelling\ ratio = \frac{W_t - W_d}{W_d} \cdot 100 \quad (1)$$

where W_t is the weight of the wet hydrogel as a function of time, and W_d is the weight of the dry one.

2.9. Rheology

Rheological analyses were performed on p-AC and f-AC systems at 37 °C using a Rheometric Scientific ARES (TA Instruments, New Castle, DE, USA) equipped with parallel plates 30 mm in diameter with a 4 mm gap in-between. These analyses were compared with AC neat hydrogels, already published in other works [38]. The oscillatory responses and dynamic frequency sweep tests (G′, elastic modulus and G′′, loss/viscous modulus) were determined at low strain values over the frequency range of 0.1–500 rad s^{-1} [38]. The thixotropic behavior of the samples was also investigated; the shear strain and viscosity as a function of shear rate were evaluated too.

2.10. NP loading with To-Pro3 and in vitro delivery

To-Pro3 (hereafter termed To-Pro, hydrodynamic radius (HR) = 7 Å, 0.7 mg mL^{-1}, Invitrogen, Italy [40]) was loaded in NPs after the polymerization reaction. Firstly, the PMMA-NP latex concentration was increased under vacuum at room temperature with the use of a rotavapor apparatus (Buchi instruments). 1 ml NPs latex at 25% w/w was obtained with the absence of aggregates, as confirmed by DLS measurements. The concentrated latex was incubated with 20 μg To-Pro3 for one day at room temperature under gentle magnetic stirring. The latex was then diluted to the desired concentration (2.5% w/w).

Loading efficiency (% loading) was calculated based on the following equation

$$\%\ loading = \frac{To - Pro3\ entrapped\ in\ NPs}{Initial\ amount\ of\ To - Pro3\ added} \times \cdot 100 \quad (2)$$

The NPs loaded with To-Pro3 at a concentration of 1% wt/wt were loaded within p-AC hydrogels and f-AC hydrogels. The samples were then placed in excess of the PBS at 37 °C, and the aliquots were collected at defined time points, while the sample volume was replaced by fresh PBS in order to avoid mass-transfer equilibrium with the surrounding solution. The supernatant of the NPs was recovered using Vivaspin 500 (Sartorius Stedim, UK). The aliquot was added to the Vivaspin 500, and the system was centrifuged at 4000 rpm for 15 min [21]. Then, the following procedure was repeated two times to ensure a complete supernatant recovery: 100 μL of deionized water was added to the Vivaspin, and the system was centrifuged at 4000 rpm for 15 min. The percentage of To-Pro3 released was measured by spectroscopy. The results were expressed as the average percentage released ± standard deviation, $n = 3$.

2.11. Statistical analysis

Where applicable, the experimental data were analyzed using Analysis of Variance (ANOVA). Statistical significance was set to p value <0.05. The results are presented as mean value ± standard deviation.

3. Results and discussion

The incorporation of NPs after hydrogel synthesis before the sol/gel transition, defined as a ‘physical’ entrapment of NPs within the AC hydrogel network (p-AC), was the first choice to control and sustain the diffusion of NPs from the hydrogel matrix. In this way a structure with NPs incorporated within

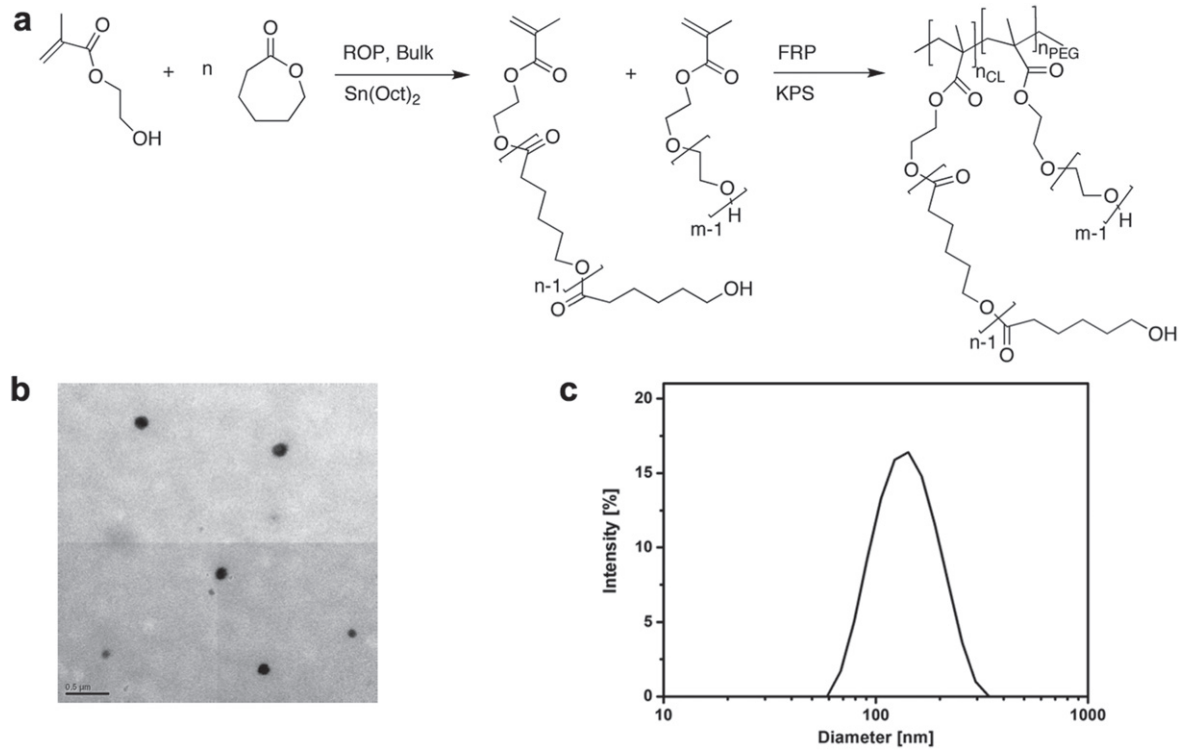

Figure 1. (**a**) Synthetic route of NPs; (**b**) TEM picture of NPs (scale bar = 500 nm); (**c**) DLS measurement of NPs.

hydrogel pores in which only steric or weak-based interactions are present can be obtained. In the case of poly(methyl methacrylate) (PMMA) NPs, release from the hydrogel matrix is completed in approximately one month, depending upon the NP diameter [38]. Conversely, the NP loading before the hydrogel synthesis allows them to be made a constitutive part of the hydrogel network, thus drastically reducing their mobility (f-AC). In particular, if NPs with hydroxyl groups (OH) on their surface are selected, they can take part in the polycondensation reaction with carbomer carboxyl groups, leading to hydrogel formation. The first experiments were performed with PMMA-based NPs or poly (lactic acid) (PLA)-based ones and synthesized as recently reported by Lazzari *et al* [41].

When PMMA-based NPs are adopted, the linking reaction takes advantage of the OH moieties present on Tween80, the emulsifier which covers the NP surface. However, such a reaction subtracts the emulsifier from the NP surface, leading to NP aggregates with an average size in the order of μm, as detected from DLS release studies (details are reported in Supporting Information—SI). Conversely, if PLA-based NPs are used, the OH end groups of the polymer can react to form hydrogel. In addition carboxyl moieties that also constitute PLA end groups may react with agarose or NPs, leading to aggregation in this case (Supporting Information). The problems were overcome by moving to biodegradable polymers possessing a comb-like structure (figure 1(a)) based on poly-ε-caprolactone (PCL) and poly ethylene glycol (PEG) chains in which each polymer repeating unit is ended with a hydroxyl group, thus forming NPs with numerous -OH moieties present on their surface without the addition of carboxyl groups [34].

As a result, NPs revealed suitable characteristics for the formation of ester bonds during the polycondensation reaction occurring within the AC synthesis since PEG chains allow the stabilization of NPs rather than acting as an emulsifier, while the very high number of hydroxyl groups allows the preservation of NP stability after the polycondensation reaction.

These NPs were obtained through a solvent-free synthesis composed of two steps summarized in figure 1(a). A ROP reaction allows us to obtain short and controllable PCL-based macromonomers, which confer the biodegradable characteristics to the NPs. The characterization of the macromonomer (i.e. ^{1}H NMR, ^{13}C NMR and SEC), which is constituted of 3 units of PCL functionalized with the 2-hydroxyethyl methacrylate (HEMA) group (HEMA-CL_3) terminating with an OH moiety, is reported in the SI. The second step involves the MMSEP of the macromonomer HEMA-CL_3; the process allows us to obtain monodispersed NPs with small and controllable size (figures 1(b)–(c)) [42]. The comb-like structure of NPs is constituted of a poly(HEMA)backbone in which each HEMA unit is grafted with PCL oligomers and PEG chains that improve NP stability and reduce opsonization in biological media (figure 1(a)) [36]. Additionally, the controllable length of the branched chains in terms of PCL units added to the HEMA molecule allows us to tune the polymer hydrophobicity and, as a result, the degradation rate of the final NPs [43]. The synthesized NPs participate in the hydrogel synthesis (f-AC) as it can be easily followed through FTIR analysis. The functional groups of agarose, carbomer

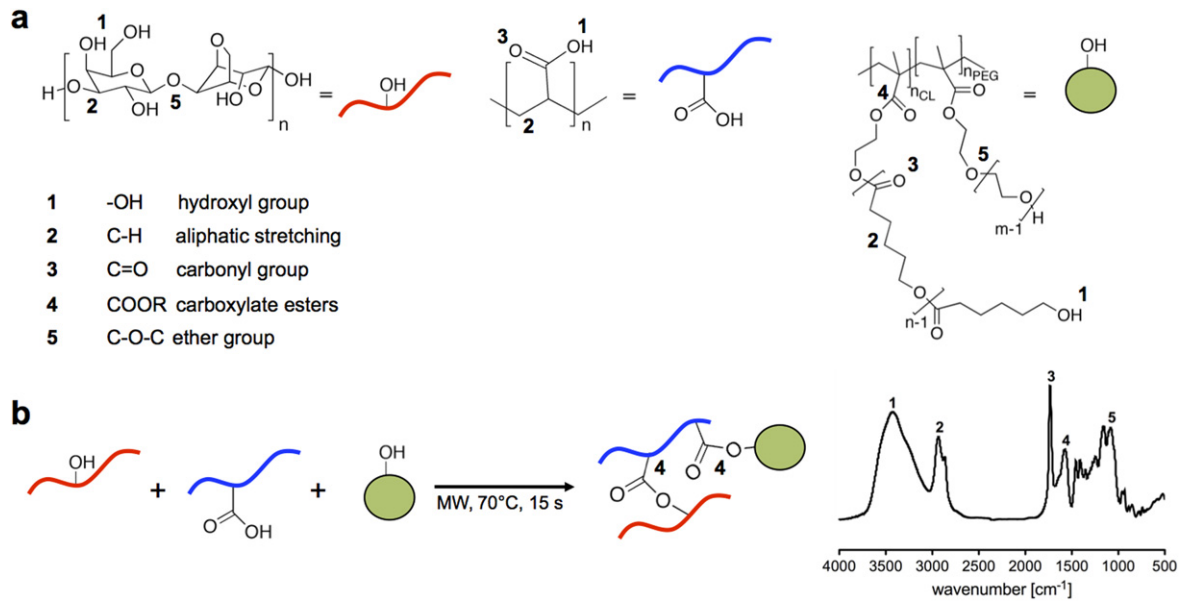

Figure 2. (**a**) Molecular structures of the involved polymers and their FTIR spectra that show the presence of –OH (**1**), C-H (**2**), C = O (**3**), COO^- (**4**) and C-O-C (**5**) groups. (**b**) f-AC hydrogel synthesis route: poly(acrylic acid) reacts with agarose and NPs (microwave radiation (MW), 70 °C, 15 s). FTIR spectrum of f-AC show the presence of AC peaks: –OH (3450 cm^{-1}, **1**), C-H (2950 cm^{-1}, **2**), COO^- (1590 cm^{-1} **4**) and C-O-C (1100 cm^{-1} **5**) with, in addition, free carbonyl groups (**3**) from the NPs.

974p and NPs, which constitute the final f-AC, are presented schematically in figure 2(a) together with their FTIR spectra.

The linking reaction between the hydrophilic polymer chains and NPs was conducted in a microwave-assisted condition in which the formation of stable structures is favored, and the single component's structure, especially in NPs, is maintained (figure 2(b)).

This phenomenon is dependent on the ability of a specific material (solvent or reagent) to absorb microwave energy and convert it into heat, allowing gel formation in less than 10 min. This procedure avoids both damage of the components and the denaturation of loaded compounds [44, 45]. In particular, f-AC hydrogels are synthesized through chemical cross-linking by microwave-assisted polycondensation between two polymers (agarose and carbomer 974p) and the NPs, instead of the glycerol and propylene glycol used in AC synthesis as cross-linking agents.

Since the NPs could be considered with no loss of generality as polymer chains with only hydroxyl groups as the reacting sites (figure 2(a)), all of these species, although constituted of macromolecules, act as monomers (hereafter called macromers) during the polycondensation reaction. Heating to 70 °C leads to a higher macromer mobility and thus enhances short-range interconnections among functional groups (i.e. carboxyl groups from carbomer 974p and hydroxyl ones from agarose and NPs). As polycondensation proceeds, the system viscosity increases continuously, decreasing the probability of interaction between distant macromer reactive sites and increasing the possibility of an efficient reaction between closer functional groups. The final result could be considered as a welding between the microgels' surfaces, giving rise to the final three-dimensional macrostructure, which is still in a liquid-like state (gelation happens at 37 °C, leading to the desired hydrogel structure). From previous studies it was evident that AC gelation occurs through carboxylate esters formation between carbomer 974p and agarose [46]. Consequently, the absence of peak 3 in the case of AC (Supporting Information, figure S7) is due to the fact that carboxyl groups are less numerous than hydroxyl ones and were totally consumed during gelation. Conversely, in the case of f-AC, C = O (1740 cm^{-1}, **3**) carbonyl groups, not present in AC hydrogel, underline the presence of NPs in the matrix and correspond to carbonyl moieties covering NPs (figure 2(b)), as reported in the literature [47].

These carbonyl groups, being part of a long PCL-based polymer chain, are less reactive than the free ones (present in carbomer 974p) and remain entrapped within the polymer network without taking part in the reaction. This happens since the esterification reaction of carboxyl groups is promoted in contrast to the transesterification reaction that involves PCL chains and OH groups. Conversely, most of the carboxyl groups of carbomer 974p (figure 2(a)) take part in the esterification reaction with agarose and are commonly visible with FTIR at wavenumbers corresponding to the $–COO^-$ group (Supporting Information, figure S7). However, it is not possible to distinguish the contributions of agarose and NPs from the FTIR spectrum (1590 cm^{-1}, 4, figure 2(a)), which underline the matrix functionalization.

A removal of free NPs before the sol/gel transition has been considered; however, if methods based on dialysis are fruitful for small molecules, such as dyes or proteins, they are not applicable to NPs due to their high molecular weight and steric hindrance. Then, as *a posteriori* proof of the occurred reaction between the hydrogel and NPs, the FTIR spectrum of f-AC was collected after the delivery studies (i.e. after one month; see below) and compared with p-AC (NPs physically

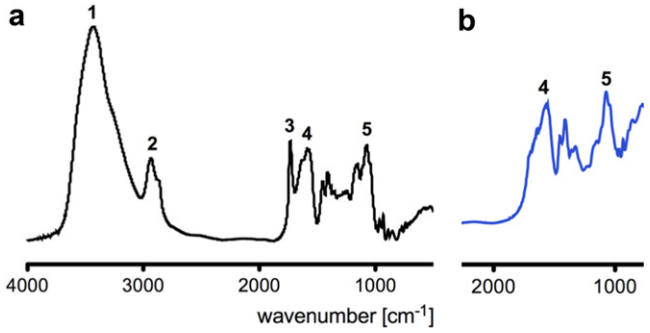

Figure 3. FTIR spectrum of the f-AC collected after delivery studies shows the presence of –OH (**1**), C-H (**2**), C = O (**3**), COO^- (**4**) and C-O-C (**5**) groups (**a**), while a detail of the FTIR spectrum of the p-AC shows the presence of peaks (**4**, **5**) while (**3**) is absent (**b**).

entrapped after the polycondensation reaction). The FTIR spectrum of f-AC reported in figure 3(a) shows the same peaks present in figure 3, underlining the functionalization of the AC hydrogel with NPs, which remain localized in the hydrogel matrix [47]. In contrast, p-AC hydrogels (figure 3(b)) do not show the presence of carbonyl groups, reported in figure 2(a) as typical of the NPs, underlining the complete leakage of NPs and thus validating the NP-hydrogel bond in f-AC.

Moreover, we have used ^{13}C HRMAS-NMR spectroscopy to obtain suitable line widths of NMR resonances of both p-AC and f-AC swollen hydrogels, in addition to the solution-state NMR of the macromonomers. The ^{13}C HRMAS-NMR spectrum of the f-AC composite, reported in figure 4, shows sharp, well-resolved lines of the terminal PEG and HEMA-CL_3 moieties.

A comparison between the ^{13}C HRMAS spectrum of the f-AC polymer (expanded region of the HEMA-CL_3 moiety) and the solution-state ^{13}C spectrum of the HEMA-CL_3 macromonomer is reported in figure 5. It is interesting to observe that the spectrum of the swollen polymer exhibits similar features of the high-resolution spectrum of the initial HEMA-CL_3 macromonomer. The complete spectral assignment has been performed using a solution-state ^1H-^{13}C 2D HSQC experiment of the HEMA-CL_3 monomer (Supporting Information, figures S3–S4), which correlates the chemical shifts of directly bound carbon-proton nuclei. The signals at 64 ppm can be assigned to the carbon (H) of the HEMA-CL_3 moiety, while the peak at 61.5 corresponds to the overlapped carbons (C) and (H′).

The peaks at 34 – 32 ppm belong to the carbons (D, D′) and carbon (G′); additional peaks detected at 28 – 23 ppm are assignable to the alkyl chain carbon (E), (F) and (G) of HEMA-CL_3. The strong peak observed at 70 ppm belongs to the terminal moieties of PEG.

The ^{13}C NMR spectrum of the f-AC composite exhibits similar homogeneous line widths for both components of the polymer PEG and the HEMA-CL_3, while the agarose backbone is not observed. The ^1H and ^{13}C NMR line widths and line shapes are related to the mobility of the species on the NMR timescale. A similar line width indicates similar molecular mobility for both components linked in the rigid polymer network. Conversely, in the ^{13}C NMR spectrum of the p-AC hydrogels (Supporting Information, figure S9), the peaks corresponding to the NP moiety are not detectable, thus providing that the physically entrapped NPs have been released.

The suitability of f-AC as an injectable hydrogel system was firstly studied in terms of gelation time, swelling kinetics and rheological behavior in comparison with AC and p-AC By the inverted test tube all of the samples gelled for less than 5 min without any kind of difference between them. The gelation phenomenon is rapid for these systems, underlining their suitability for biomedical applications.

The ability to absorb and retain a large amount of water, evaluated as the swelling equilibrium ratio, is one of the most important features for 3D polymeric networks, such as hydrogel systems. All of the samples exhibited fast swelling kinetics, and they reached swelling equilibrium within the first hour; their swelling equilibrium values are around 4500% for AC, 2500% for f-AC and 2100% for p-AC It is well observable that, as published in the previous work [46], the swelling phenomenon exhibits a high dependence on the solute loaded within the polymeric network. In particular, its value decreases from the condition of the neat AC hydrogel to f-AC and then p-AC: this is probably caused by the hindrance that NPs are opposite to the swelling of polymer chains. In f-AC hydrogels this opposition is weaker since NPs are linked and not able to diffuse within the polymeric network. Moreover, another key point is represented by the difference in the cross-linking density between p-AC and f-AC samples: p-AC, being more cross-linked, present a weaker swelling equilibrium ratio. Regarding rheological studies, in figure 6(a), the storage modulus, G′, was compared to the unloaded gel samples AC, p-AC and f-AC in order to investigate the effect of NPs. In previous works gel storage modulus (G′) was found to be approximately one order of magnitude higher than the loss modulus (G′′), indicating an elastic rather than viscous material [48], and both of them were essentially independent from the frequency. It is well visible that the presence of NPs within the polymeric network, entrapped or bonded, does not affect the rheological properties of the composite material, which is in accordance with the previous work [38]. Comparing the neat system with p-AC and f-AC the G′ increment is evident: specifically, it results in a threefold increase for f-AC and a fourfold increase for p-AC over the neat AC hydrogel. The composite material presents stiffer and more elastic properties with respect to the AC hydrogel that could be attributed to the interactions between the AC network and PCL-based NPs. Indeed, both the NPs and hydrogel network possess negative charges, and electrostatic repulsion could take place, increasing the chain mobility and consequently the system properties. In the case of f-AC these interactions are weaker since NPs do not have the possibility to move; so, the composite material presents, with respect to p-AC, lower G′ values.

The monotonic enhancement in hydrogel mechanical properties for p-AC and f-AC suggests also that NPs are well dispersed within the AC polymeric matrix and do not create heterogeneous spots all along the hydrogel. Figure 6(b) shows

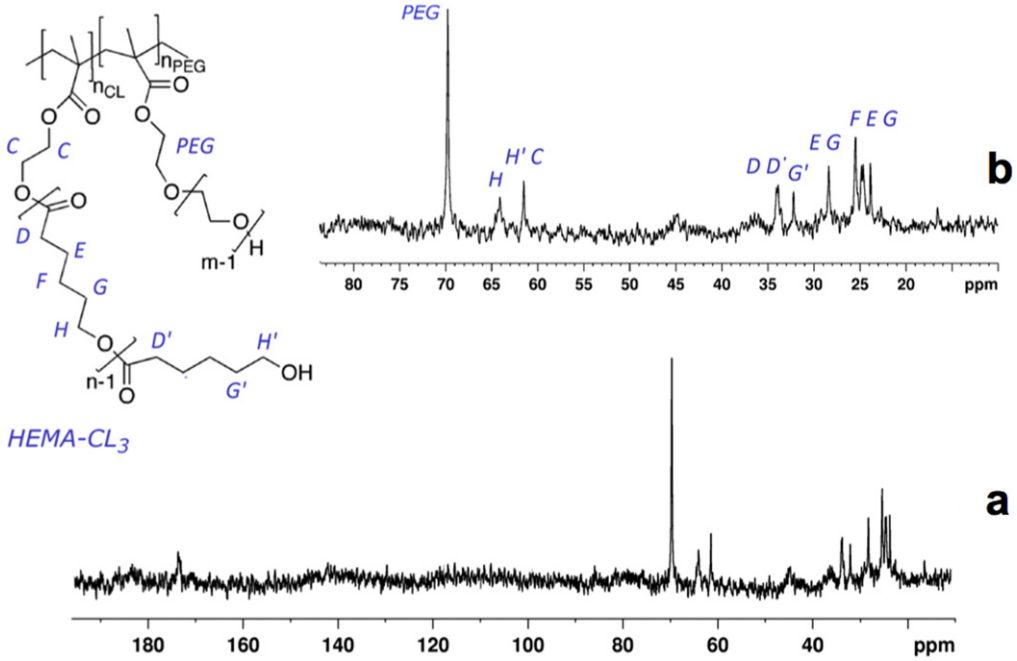

Figure 4. ^{13}C HRMAS spectra of the f-AC polymer (**a**) and the (0–85 ppm) expanded region (**b**), along with a representative molecular formula and atom numbering of the polymer chains constituting the NPs.

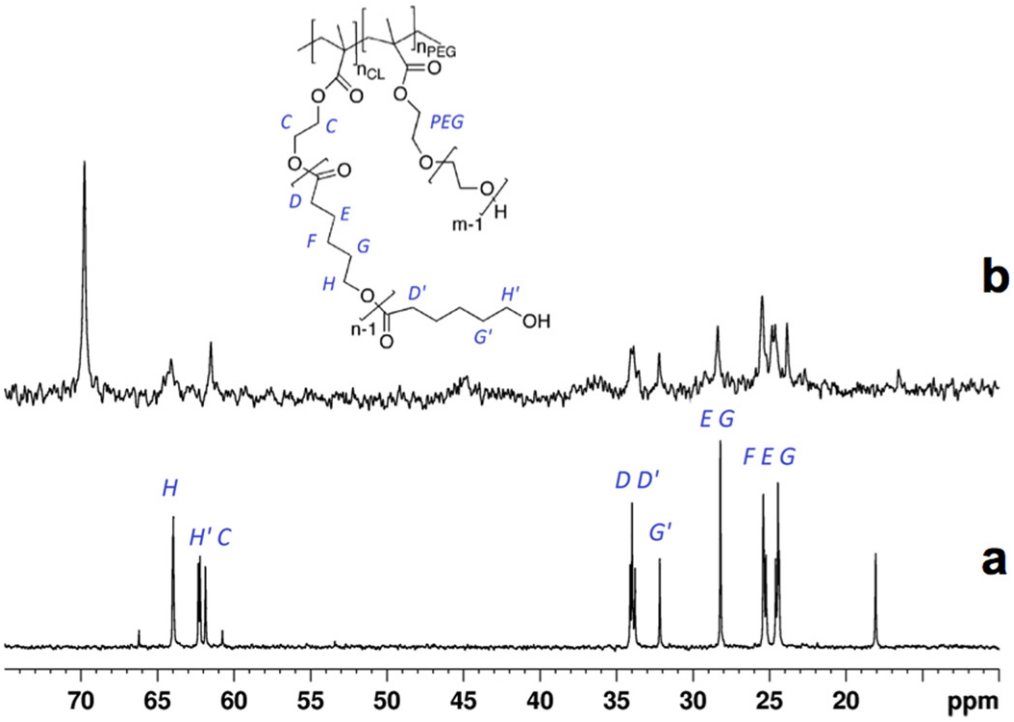

Figure 5. ^{13}C high-resolution spectrum of the HEMA-CL_3 macromonomer (0–85 ppm expanded region) (**a**) and ^{13}C HRMAS spectrum of the f-AC polymer (**b**).

shear behavior plots of AC, p-AC and f-AC gels, each presenting the typical hysteresis loop, a distinguishing mark of thixotropic materials. As is well known, the area within the hysteresis loop represents the energy loss required to obtain the sol-gel transition and is directly linked to the time necessary for material rearrangement [49]. The investigated formulations showed thixotropy at low shear rate values, and the presence of NPs increases the loop area, makes the gels more stable and leads to higher mechanical properties, which is in agreement with the dynamic frequency sweep tests.

After we had proved the f-AC composite formation, we studied the effective and lasting NP localization at the injection site and the possibility to sustain drug delivery. In particular, it should be underlined that NPs directly injected

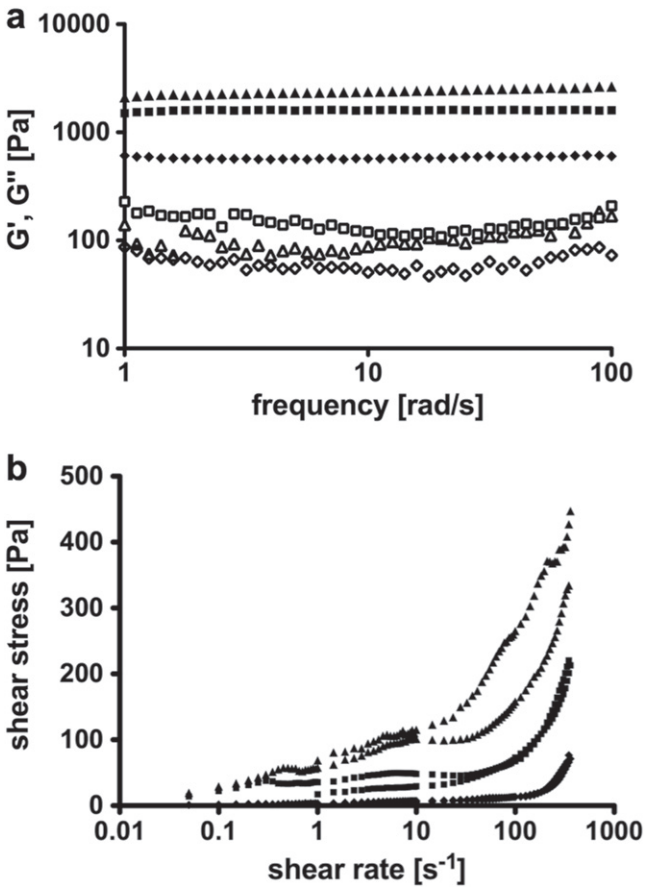

Figure 6. Rheological analyses: (**a**) dynamic frequency sweep test of p-AC, f-AC and AC hydrogels at 37 °C with small oscillatory shear in the linear viscoelastic regime: G′ (p-AC (▲), f-AC (■), AC (◆)), G″ (△ p-AC, □ f-AC, ◇ AC) (**b**). Thixotropic loop for: p-AC (▲), f-AC(■) and AC (◆).

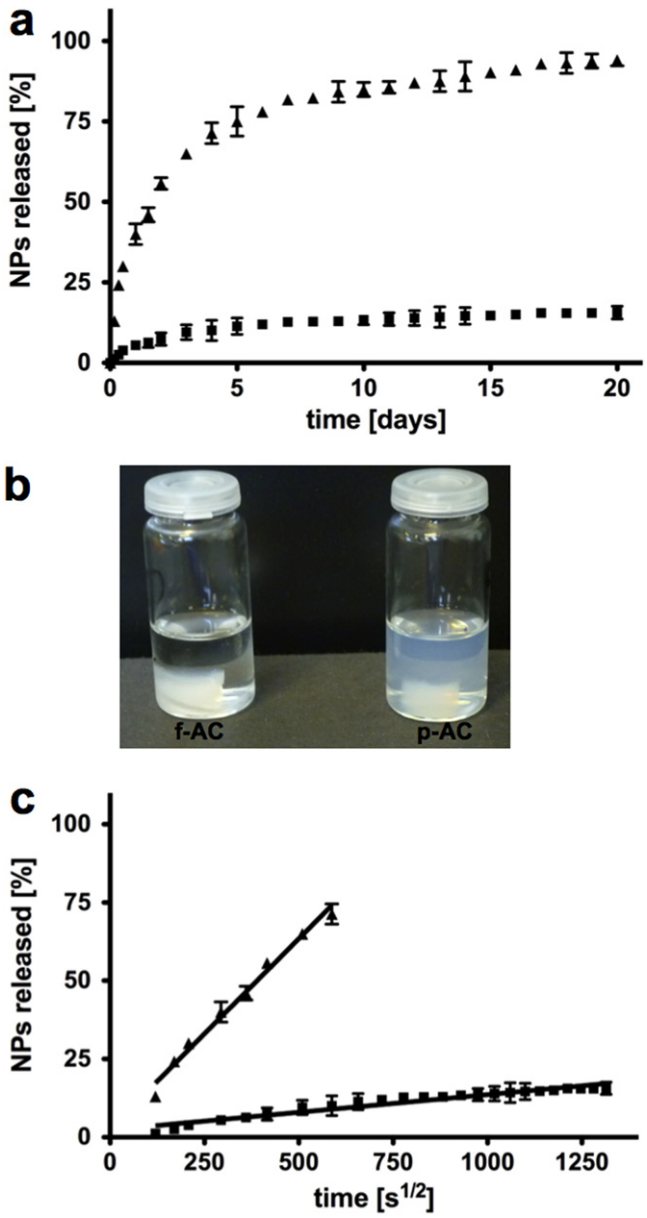

Figure 7. (**a**) *In vitro* release profile of NPs delivered from p-AC (▲) and f-AC (■) hydrogels. (**b**) f-AC and p-AC hydrogel samples after 14 days in PBS at 37 °C. The opacity of the supernatant underlining the presence of NPs is well visible in p-AC (**c**) The slope of the NP release from p-AC (▲) and f-AC (■) against the square root time is representative of the Fickian diffusion coefficient of NPs in gels ($p < 0.0001$ between all of the groups). The diffusion-controlled release is sustained for 4 days from p-AC and for 20 days from f-AC hydrogels. The values are calculated as a percentage with respect to the total mass loaded (mean value ± standard deviation is plotted).

are quickly internalized by macrophages (i.e. a few hours) [23, 50]. So, the controlled release of drug-loaded NPs from hydrogels could help to both sustain a selective and effective release of drugs and delay the cell uptake mechanism.

As expected, the high diffusivity rate of NPs might seem to be the major limit of the technique; thus, after a proper calibration of DLS (Supporting Information, figure S10), we evaluated the amount of NPs released from the system over time. In order to verify the effective NPs-AC bond, the release of NPs from f-AC hydrogels was compared with p-AC From the first inspection, the release of NPs from AC alone was nearly complete after 14 days, thus validating the FTIR data, whereas the release from the f-AC hydrogel is only partial even after 20 days, as clearly detectable in figure 7(a).

From a physical point of view, multiple mechanisms can explain these events; thus, the release from f-AC as well as the diffusion of the NPs non-linked within the polymer matrix can occur by hydrolytic rupture of hydrogel-polymer ester bonds and also with the partial NP degradation, which follows a hydrolytic mechanism. In fact, the degradation process occurs through a swelling mechanism and the further hydrolysis of the branched chains, followed by a PCL oligomer release and their degradation to 6-hydroxycaproic acid. Once the branched chains are completely released it remains a poly(HEMA) chain which, being hydrophilic, can be easily disposed [43]. As a consequence, not only the rupture of the bonds between NPs and hydrogel but also the degradation of the NP side chains can explain the NP release, which is indeed lower than 15% of the loaded NPs after 20 days. The fastest release for physically entrapped NPs confirms the hypothesis that tunable release profiles could be achieved by

functionalizing AC with NPs. Moreover, the initial burst release, which is relevant in the case of NPs entrapped into a hydrogel matrix, which can be attributed to the high initial concentration gradient and in particular to the NPs that are closer to the solvent-hydrogel interface, is significantly limited using f-AC. That result clearly indicates that NP diffusivity, which dominates for p-AC, is drastically reduced for f-AC.

This is also very visible from a qualitative point of view in figure 7(b), where the opacity of the supernatant underlines the presence of NPs only in the p-AC sample.

Then, to study differences in the diffusion coefficient of NPs in the two different AC hydrogels (p-AC and f-AC) we plotted the release against the square root of time ($t^{1/2}$, figure 7(c)), where a linear relationship is indicative of Fickian diffusion [50]. By comparing the slopes in the linear region for p-AC and f-AC hydrogels it is visible that the relative diffusion coefficient is extremely different for the two cases ($p < 0.0001$). For p-AC the data fit linearly for 4 days of release, while for f-AC, it fit all of the times it was involved in the study. These results confirm that the release from f-AC hydrogels is still mediated by Fickian diffusion. This linear trend means the burst release attributed to NPs close to the gel interface is overcome in the case of physically loaded NPs and furnishes another indirect proof of the matrix functionalization since the rate of diffusion-controlled release is drastically reduced.

To further understand the suitability of these composite release systems as drug delivery devices, NPs were loaded with To-Pro before being included within AC hydrogels. To-Pro is a far-red fluorophore, used here as a drug mimetic compound [21]. The loading percentage of To-Pro within the NPs was 84 ± 3%, as detected by spectroscopy. The release of To-Pro from f-AC and p-AC was investigated after incubating the samples at 37 °C and is presented in figure 8. In both cases To-Pro release, as shown in figure 8(a), followed a biphasic pattern characterized by an initial burst release, followed by a slower sustained release phase that was observed during the 21 days. From figure 8(b) the pure Fickian diffusion phenomenon is evident where a linear relationship between the percentage released and square root time was observed. These results confirm that the release from both the p-AC and f-AC is still mediated by Fickian diffusion.

The percentage of To-Pro released in the first 2 h is around 25% for p-AC and 14% for f-AC In the case of p-AC the burst value can be attributed to both the unloaded To-Pro and to the high initial concentration gradient. Conversely, for f-AC we have a smaller released value due to the presence of immobilized NPs that are not able to move across the hydrogel network. Thereon, To-Pro was slowly released with a comparable trend between p-AC and f-AC, underlining the possibility to sustain the release of drugs in a similar way with different systems, depending on the pharmacological approach. On one side p-AC could deliver drugs selectively to specific cell lines [20, 38], while on the other side, f-AC could sustain the release of drugs with a low burst release and remain immobilized within a polymeric network.

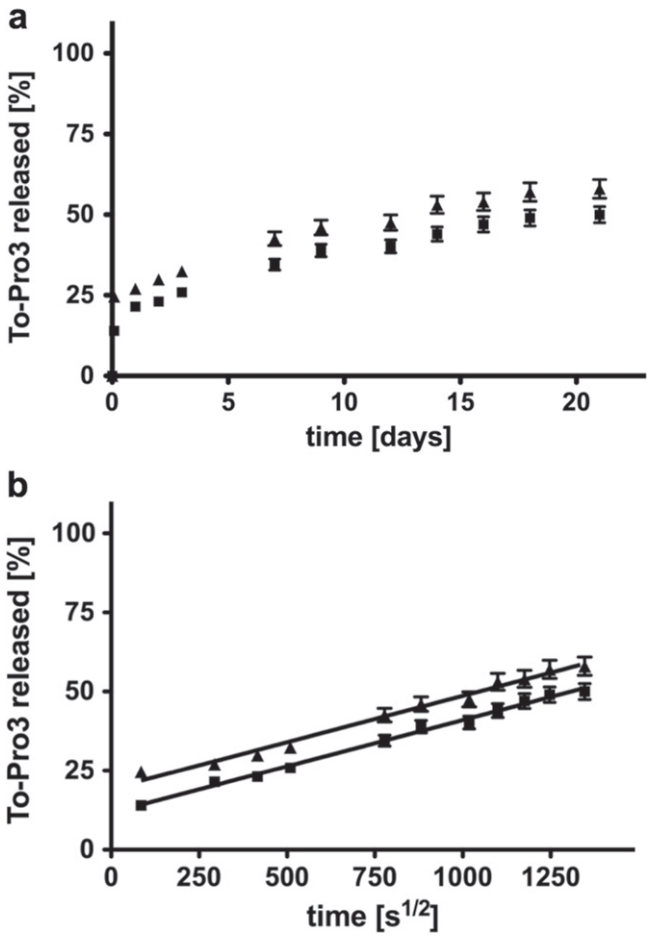

Figure 8. (**a**) *In vitro* release profile of To-Pro delivered from p-AC (▲) and f-AC (■). (**b**) The slope of the To-Pro release from p-AC (▲) and f-AC (■) against the square root time is representative of the Fickian diffusion coefficient of NPs in gels ($p < 0.0001$ between all of the groups). The diffusion-controlled release is sustained from both the p-AC and f-AC hydrogels. The values are calculated as a percentage with respect to the total mass loaded (mean value ± standard deviation is plotted).

4. Conclusions

In this study a novel composite material made of cross-linked hydrogel functionalized with biodegradable polymer NPs has been proposed. This system is able to significantly limit NP diffusion during the time joining the different peculiarities of both hydrogels and polymer NPs. It is aimed at optimizing drug therapies in which the release of hydrophobic compounds, otherwise selectively directed to specific cell lines, is able to stay localized at the injection site. This work, in conjunction with previous studies, aims to build a material library able to provide different release rates and different release alternatives while maintaining the same material skeleton.

Thus, such composite materials can find unique applications in cartilage or bone tissue engineering, neurological disease, spinal cord injury or tissue repair. Moreover, these novel composites can be profitably adopted when active agents should be released with independent kinetics.

Acknowledgment

This study was supported by Fondazione Cariplo, grant no. 2010/0639. We are grateful to Professor Maurizio Masi for fruitful discussions.

SUPPLEMENTARY DATA

NPs and hydrogel characterization studies (FTIR, HRMAS-NMR and DLS) are collected in the Supporting Information.

References

[1] Wolinsky J B, Colson Y L and Grinstaff M W 2012 Local drug delivery strategies for cancer treatment: gels, nanoparticles, polymeric films, rods, and wafers *J. Control Release* **159** 14–26

[2] Shi J, Votruba A R, Farokhzad O C and Langer R 2010 Nanotechnology in drug delivery and tissue engineering: from discovery to applications *Nano Lett.* **10** 3223–30

[3] Yuan L, Tang Q Q, Yang D, Zhang J Z, Zhang F Y and Hu J H 2011 Preparation of pH-responsive mesoporous silica nanoparticles and their application in controlled drug delivery *J. Phys. Chem.* C **115** 9926–32

[4] Saltzman W M 2001 *Drug Delivery: Engineering Principles for Drug Therapy* (New York, USA: Oxford University Press)

[5] Bajpai A K, Shukla S S, Bhanu S and Kankane S 2008 Responsive polymers in controlled drug delivery *Prog. Polym. Sci.* **33** 1088–118

[6] Siepmann J and Siepmann F 2012 Modeling of diffusion controlled drug delivery *J. Control Release* **161** 351–62

[7] GhoshMitra S, Diercks D R, Mills N C, Hynds D and Ghosh S 2012 Role of engineered nanocarriers for axon regeneration and guidance: current status and future trends *Adv. Drug Deliv. Rev.* **64** 110–25

[8] Baumann M D, Kang C E, Tator C H and Shoichet M S 2010 Intrathecal delivery of a polymeric nanocomposite hydrogel after spinal cord injury *Biomaterials* **31** 7631–9

[9] Rossi F, Perale G, Papa S, Forloni G and Veglianese P 2013 Current options for drug delivery to the spinal cord *Expert Opin. Drug Deliv.* **10** 385–96

[10] Nicolas J, Mura S, Brambilla D, Mackiewicz N and Couvreur P 2013 Design, functionalization strategies and biomedical applications of targeted biodegradable/ biocompatible polymer-based nanocarriers for drug delivery *Chem. Soc. Rev.* **42** 1147–235

[11] Bertrand N, Wu J, Xu X Y, Kamaly N and Farokhzad O C 2014 Cancer nanotechnology: the impact of passive and active targeting in the era of modern cancer biology *Adv. Drug Deliv. Rev.* **66** 2–25

[12] Kuo Y C and Ko H F 2013 Targeting delivery of saquinavir to the brain using 83-14 monoclonal antibody-grafted solid lipid nanoparticles *Biomaterials* **34** 4818–30

[13] Canton I and Battaglia G 2012 Endocytosis at the nanoscale *Chem. Soc. Rev.* **41** 2718–39

[14] Gu Z *et al* 2013 Injectable nano-network for glucose-mediated insulin delivery *ACS Nano* **7** 4194–201

[15] Otsuka H, Nagasaki Y and Kataoka K 2012 PEGylated nanoparticles for biological and pharmaceutical applications *Adv. Drug Deliv. Rev.* **64** 246–55

[16] Wei K, Peng X M and Zou F 2014 Folate-decorated PEG-PLGA nanoparticles with silica shells for capecitabine controlled and targeted delivery *Int. J. Pharm.* **464** 225–33

[17] Kim Y T, Caldwell J M and Bellamkonda R V 2009 Nanoparticle-mediated local delivery of methylprednisolone after spinal cord injury *Biomaterials* **30** 2582–90

[18] Shoichet M S 2010 Polymer scaffolds for biomaterials applications *Macromolecules* **43** 581–91

[19] Li X Y, Zhang Z L and Chen H 2013 Development and evaluation of fast forming nano-composite hydrogel for ocular delivery of diclofenac *Int. J. Pharm.* **448** 96–100

[20] Papa S *et al* 2013 Selective nanovector mediated treatment of activated proinflammatory microglia/macrophages in spinal cord injury *ACS Nano* **7** 9881–95

[21] Papa S *et al* 2014 Polymeric nanoparticle system to target activated microglia/macrophages in spinal cord injury J. *Control Release* **174** 15–26

[22] Jain N K, Mishra V and Mehra N K 2013 Targeted drug delivery to macrophages *Expert Opin. Drug Deliv.* **10** 353–67

[23] Sharma G *et al* 2010 Polymer particle shape independently influences binding and internalization by macrophages J. *Control Release* **147** 408–12

[24] Smith D M, Simon J K and Baker J R 2013 Applications of nanotechnology for immunology *Nat. Rev. Immuno* **13** 592–605

[25] Champion J A and Mitragotri S 2006 Role of target geometry in phagocytosis *Proc. Natl. Acad. Sci. USA* **103** 4930–4

[26] Doggui S, Sahni J K, Arseneault M, Dao L and Ramassamy C 2012 Neuronal uptake and neuroprotective effect of curcumin-loaded PLGA nanoparticles on the human SK-N-SH cell line *J. Alzheimers Dis.* **30** 377–92

[27] Wu J, Wu D Q, Mutschler M A and Chu C C 2012 Cationic hybrid hydrogels from amino-acid-based poly(ester amide): fabrication, characterization, and biological properties *Adv. Func. Mater.* **22** 3815–23

[28] Cho E C, Kim J-W, Fernandez-Nieves A and Weitz D A 2008 Highly responsive hydrogel scaffolds formed by three-dimensional organization of microgel nanoparticles *Nano Lett.* **8** 168–72

[29] Molinos M, Carvalho V, Silva D M and Gama F M 2012 Development of a hybrid dextrin hydrogel encapsulating dextrin nanogel as protein delivery system *Biomacromolecules* **13** 517–27

[30] Liu J *et al* 2007 Controlled release of insulin from PLGA nanoparticles embedded within PVA hydrogels *J. Mater. Sci-Mater. Med.* **18** 2205–10

[31] Stanwick J C, Baumann M D and Shoichet M S 2012 Enhanced neurotrophin-3 bioactivity and release from a nanoparticle-loaded composite hydrogel *J. Control Release* **160** 666–75

[32] Yildirimer L, Thanh N T K, Loizidou M and Seifalian A M 2011 Toxicological considerations of clinically applicable nanoparticles *Nano Today* **6** 585–607

[33] Ferrari R *et al* 2013 Synthesis of surfactant free PCL-PEG brushed nanoparticles with tunable degradation kinetics *Int.* J. *Pharm.* **453** 551–9

[34] Ferrari R, Yu Y C, Morbidelli M, Hutchinson R A and Moscatelli D 2011 Epsilon-caprolactone-based macromonomers suitable for biodegradable nanoparticles synthesis through free radical polymerization *Macromolecules* **44** 9205–12

[35] Perale G *et al* 2012 Multiple drug delivery hydrogel system for spinal cord injury repair strategies *J. Control Release* **159** 271–80

[36] Ferrari R, Yu Y, Lattuada M, Storti G, Morbidelli M and Moscatelli D 2012 Controlled PEGylation of PLA-based nanoparticles *Macromol. Chem. Phys.* **213** 2012–8

[37] Santoro M *et al* 2011 Smart approach to evaluate drug diffusivity in injectable agar-carbomer hydrogels for drug delivery *J. Phys. Chem.* B **115** 2503–10

[38] Rossi F *et al* 2013 Tunable hydrogel—nanoparticles release system for sustained combination therapies in the spinal cord *Colloid Surf.* B **108** 169–77
[39] Gupta D, Tator C H and Shoichet M S 2006 Fast-gelling injectable blend of hyaluronan and methylcellulose for intrathecal, localized delivery to the injured spinal cord *Biomaterials* **27** 2370
[40] Prodhomme S, Demaret J P, Vinogradov S, Asseline U, Morin-Allory L and Vigny P 1999 A theoretical and experimental study of two thiazole orange derivatives with single- and double-stranded oligonucleotides, polydeoxyribonucleotides and DNA *J. Photochem. Photobiol. B: Biol.* **53** 60–9
[41] Lazzari S, Moscatelli D, Codari F, Salmona M, Morbidelli M and Diomede L 2012 Colloidal stability of polymeric nanoparticles in biological fluids *J. Nanopart. Res.* **14** 920
[42] Dossi M *et al* 2012 Synthesis of fluorescent PMMA-based nanoparticles *Macromol. Mat. Eng.* **298** 771–8
[43] Ferrari R, Colombo C, Dossi M and Moscatelli D 2013 Tunable PLGA-based nanoparticles synthesized through free-radical polymerization *Macromol. Mat. Eng.* **298** 730–9
[44] Kappe C O 2004 Controlled microwave heating in modern organic synthesis *Angew Chem. Int. Edn.* **43** 6250–84
[45] Kushare S S and Gattani S G 2013 Microwave-generated bionanocomposites for solubility and dissolution enhancement of poorly water-soluble drug glipizide: *in-vitro* and *in-vivo* studies *J. Pharm. Pharmacol.* **65** 79–93
[46] Rossi F, Santoro M, Casalini T, Veglianese P, Masi M and Perale G 2011 Characterization and degradation behavior of agar—carbomer based hydrogels for drug delivery applications: solute effect *Int. J. Mol. Sci.* **12** 3394–408
[47] Elzein T, Nasser-Eddine M, Delaite C, Bistac S and Dumas P 2004 FTIR study of polycaprolactone chain organization at interfaces *J. Colloid Interface Sci.* **273** 381–7
[48] Jiang J *et al* 2008 Rheology of thermoreversible hydrogels from multiblock associating copolymers *Macromolecules* **41** 3646–52
[49] Barbucci R, Pasqui D, Favaloro R and Panariello G 2008 A thixotropic hydrogel from chemically cross-linked guar gum: synthesis, characterization and rheological behaviour *Carbohyd. Res.* **343** 3058–65
[50] Vulic K and Shoichet MS 2012 Tunable growth factor delivery from injectable hydrogels for tissue engineering *J. Am. Chem. Soc.* **134** 882–5